A new look at bearing signal models

W.A. Smith[1], P. Borghesani[1], D. Abboud[2], R.B. Randall[1], J. Antoni[3], M. El Badaoui[2], Z. Peng[1]
[1] UNSW Sydney, School of Mechanical and Manufacturing Engineering,
NSW 2052, Australia
e-mail: **wade.smith@unsw.edu.au**

[2] Safran Tech,
Rue des Jeunes Bois –Châteaufort 78772 Magny–les–Hameaux, France

[3] Univ Lyon, INSA Lyon, LVA, EA677,
69621 Villeurbanne, France

Abstract
It has been 20 years since detailed cyclostationary (CS) and pseudo-cyclostationary (PCS) bearing signal models superseded the well-known periodic models of the mid-1980s. These CS models finally provided the justification for the use of the envelope spectrum as the primary diagnostic tool, despite this having been widely appreciated by diagnosticians for several decades. Yet there have been few further developments in signal modelling in the intervening years, while diagnostic methods have advanced significantly in that time. While these (stochastic) CS models have been widely accepted, many of their features are not well understood. This paper takes a fresh look at such models and examines them in detail. Several of their key (often misunderstood) features are explained, and their underlying physical assumptions outlined. The paper then presents a newer mixed signal model, with both CS and PCS properties, and shows application of this model to laboratory measurements from degradation tests on a bearing rig. It is hoped the paper will enable the development of improved algorithms for bearing diagnostics and prognostics.

1 Introduction

The field of bearing diagnostics has come a long way since McFadden and Smith proposed their famous 'single point defect' bearing signal model in the mid-1980s [1]. At that time, the 'high frequency resonance technique' – involving the demodulation of a high frequency band, understood to be a system resonance potentially excited by a bearing fault, followed by envelope analysis – was well established. Techniques to select this band – a major topic of research over the last decade or two – were however still immature.

About 15 years later, the concept of cyclostationarity, until then understood only in niche signal processing circles, made its way into the machine diagnostics field. McCormick and Nandi [2] and Capdessus et al. [3] were the earliest adopters, both explaining the value in applying cyclostationary (CS) signal models to diagnostic problems in rotating machinery. Soon after, Randall et al. [4] made the explicit connection between cyclostationarity and envelope analysis, explaining that the envelope spectrum amounts to the integration of the spectral correlation along the carrier frequency axis, leaving a spectrum of amplitude vs cyclic frequency, rich in diagnostic information. While the value of the envelope spectrum as a crucial diagnostic tool had been appreciated for decades, its connection with the new concept of cyclostationarity had not, until then, been thoroughly understood. This connection paved the way for many further developments.

Signal models are valuable for diagnostic purposes as they allow complex signals to be meaningfully represented using only a small number of parameters that can often be tied directly to physical phenomena and sometimes even to the condition of the machine components. This allows for the development of optimal

signal processing tools and algorithms tailored to specific signal characteristics, a good example being the exploitation in recent years of cyclostationarity as a diagnostic indicator of faulty bearings, helping in the selection of the optimal frequency band for demodulation [5-8].

This paper takes a new look at the bearing signal models proposed over the last four decades – from McFadden and Smith's periodic model [1], to the purely CS 'jitter' model of Randall et al. [4] and Antoni and Randall's [9, 10] pseudo-CS 'slip' model, finishing with the recently proposed mixed CS/PCS model of Borghesani et al. [11]. The paper explains the differences in the underlying physical assumptions associated with each model, as well as the resulting statistical properties of each. Finally, an application is presented of the mixed model to signals obtained from run-to-failure tests of a bearing mounted on a laboratory test bench.

The remainder of this paper is arranged as follows. The various bearing signal models – periodic, cyclostationary ('jitter'), pseudo-cyclostationary, and a new mixed model – are described in Section 2. Section 3 describes the methodology employed to produce the results in Section 4. In Section 5, conclusions are given and topics for future work are canvassed.

2 Bearing signal models

This section discusses the properties of four bearing signal models: periodic, cyclostationary ('jitter'), pseudo-cyclostationary, and a recently proposed mixed CS/PCS model. We begin with the general model of a bearing signal:

$$x(t) = \sum_{k=-\infty}^{\infty} A_k s(t - T_k). \tag{1}$$

in which the parameters A_k and T_k, the amplitude and timing properties of the pulses, $s(t)$, generated by a faulty rolling element bearing, are described in Figure 1. The amplitudes A_k are modelled as independent identically distributed (i.i.d.) Gaussian samples with mean μ_A and variance σ_A^2. However, the emphasis in the following will be on the timing statistics captured by T_k. For simplicity, no consideration is given here to modulation effects associated with passage of the rolling elements through the load zone.

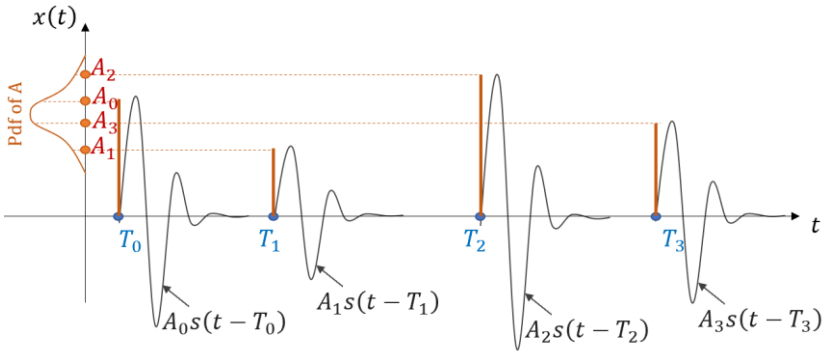

Figure 1: Illustration of terms used in bearing signal models [11]

2.1 Timing properties of the different models

2.1.1 Periodic model

In the periodic model of McFadden and Smith [1], the impact times $T_k = k \cdot T$, such that each pulse occurs exactly T seconds after the previous and thus the timing of each pulse is deterministically known. The period T is known exactly ($1/\text{BPFO}$ for an outer race fault), and, with no cage slip and no jitter of the rolling elements within the clearance of the cage, there is no randomness in the pulse timing properties.

2.1.2 Cyclostationary (CS) 'jitter' model

The CS 'jitter' model proposed by Randall et al. [4] accounts for the fact that the rolling elements are each allowed to move circumferentially within the cage clearance, adding a small randomness to the location of each rolling element as it interacts with the fault. This randomness in location produces a random delay/advance in the pulse timing τ_k called 'jitter'. This results in a truly CS bearing signal model, where the impact times are $T_k = kT + \tau_k$. This jitter τ_k is modelled as another i.i.d. Gaussian process, with zero mean and variance σ_τ^2.

One interesting feature of the randomness of this phenomenon is that jitter in one pulse does not carry over to the next, and so there is no accumulation in the uncertainty of future arrival times. Regardless of whether two pulses are consecutive or 100 pulses apart, the randomness of the distance between them only depends on the jitter of the two pulses.

2.1.3 Pseudo-cyclostationary model

Soon after the CS model of Randall et al. [4], Antoni and Randall [9, 10] introduced a pseudo-cyclostationary signal based on cage slip, representing the combined slip of the rolling elements. In this model, the speed of the cage itself varies stochastically in comparison with the ideal kinematic (no slip) model, creating a random delay/advance in pulse timing that 'carries over' from one pulse to the next – i.e., if one pulse is 'late', the next is more likely to be late as well. In this case, the time lags between subsequent pulses are given by $\Delta T_k = T_k - T_{k-1}$, which again are modelled as i.i.d. Gaussian quantities with mean $\mu_\Delta \approx T$ and variance σ_Δ^2. Note that with the PCS model, unlike with jitter, the mean pulse interval μ_Δ deviates from the theoretical value, and the variance of the time-difference between any two pulses becomes proportional to their distance in time, i.e., the uncertainty of arrival times accumulates over time.

2.1.4 New mixed model

As explained by Borghesani et al. [11], the underlying physical causes behind the CS and PCS models – jitter and cage slip – are entirely justifiable, and in fact there is no reason why the two should not co-exist in the same signal. In that paper, a mixed CS/PCS model was developed based on a hidden variable t_k, the impact time if there was no clearance/jitter (only due to cage slip), which follows the pseudo-CS model:

$$t_k = t_{k-1} + \Delta t_k, \tag{2}$$

with $\Delta t_k \sim \mathcal{N}(\mu_\Delta, \sigma_\Delta^2)$ i.i.d.. An additive zero-mean jitter τ_k due to cage-clearance then results in the observed pulse timing T_k:

$$T_k = t_k + \tau_k, \tag{3}$$

with $\tau_k \sim \mathcal{N}(0, \sigma_\tau^2)$ i.i.d.. This results in variance of the time-difference between any two pulses linearly growing with their distance in time, but starting from an offset:

$$(T_{k+n} - T_k) \sim \mathcal{N}\left(n\mu_\Delta, |n|\sigma_\Delta^2 + 2\sigma_\tau^2 \cdot \left(1 - \delta_{n,0}\right)\right). \tag{4}$$

The differences in timing statistics and pulse timing uncertainty between the four models is illustrated in Figure 2 and Figure 3.

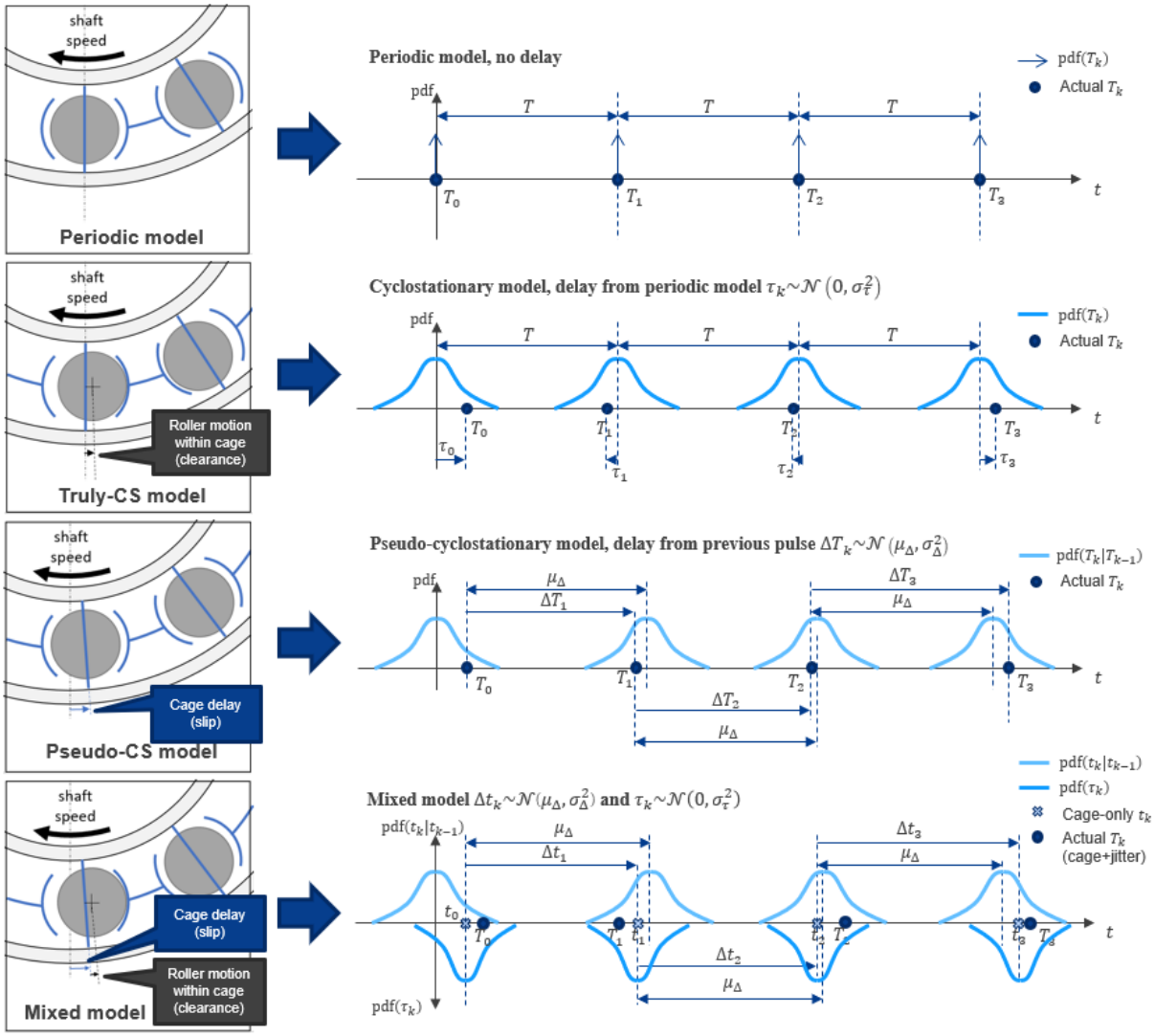

Figure 2: Timing statistics of different bearing signal models [11]

2.2 Spectral properties of the different models

2.2.1 Periodic model

The purely periodic model produces an entirely deterministic signal characterised by discrete spectral components [1]. Despite still sometimes being employed, its usefulness in the development of new diagnostic tools and methods is somewhat limited as it does not reflect the complexities of bearing signals measured in practice.

2.2.2 Cyclostationary (CS) 'jitter' model

As explained in [11], the jitter model gives a frequency spectrum dominated in the low frequency region by truly periodic components and in the high frequency region by random content. [11] gives guidelines on calculating the crossover frequency at which the random part becomes dominant. The model will not be applied in this paper, however, and so further details are omitted.

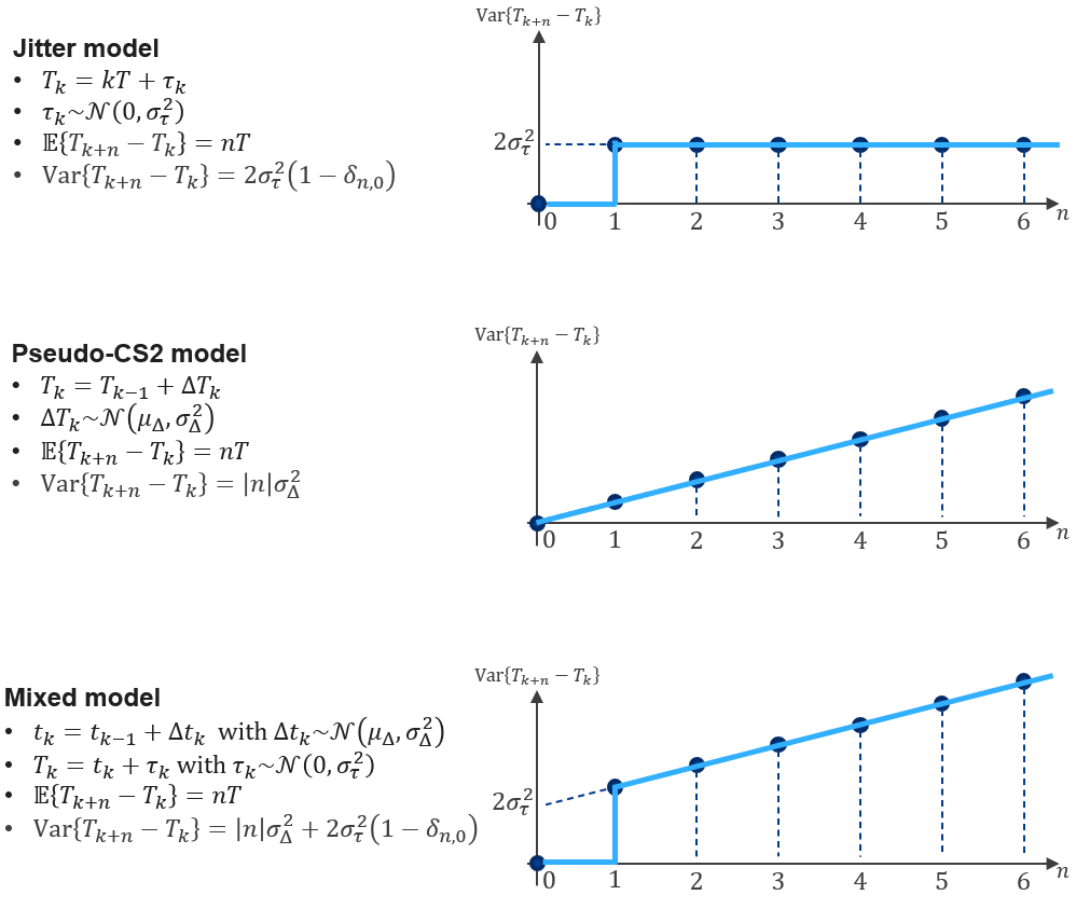

Figure 3: Variance of pulse timing vs number of pulse periods for different bearing signal models [11]

2.2.3 Pseudo-cyclostationary model

Unlike the two previous models, the PCS model gives a spectrum that has no deterministic components. Its power spectral density (PSD) is given by:

$$\mathbb{E}\{PSD_x(f)\} = \frac{|S(f)|^2}{\mu_\Delta} \cdot \mu_A^2 \cdot \left\{ \frac{\sinh(2\sigma_\Delta^2 \pi^2 f^2)}{\cosh(2\sigma_\Delta^2 \pi^2 f^2) - \cos(2\pi f / f_T)} + \frac{\sigma_A^2}{\mu_A^2} \right\}, \tag{5}$$

where μ_Δ is the actual mean bearing fault period, differing from the theoretical value T due to cage slip (unlike with the periodic and CS models, where the fault period does not vary from T). Figure 4 gives a graphical representation of eq. (5), under the simplifying case of flat $|S(f)|$, for $\sigma_\Delta = 5\%\, T$ and $\sigma_A = 10\%\, \mu_A$.

In [11] a number of detailed observations are made of the PSD in Figure 4, but most important here is the point that the peaks in the spectrum (fault frequency 'harmonics', but strictly narrow band noise) will grow broader with harmonic order. An approximate half-power bandwidth of the *n*-th peak is:

$$\frac{\Delta f_n}{f_T} \approx 2\cos^{-1}\left(2 - \cosh\left(2\pi^2 n^2 \sigma_\Delta^2 f_T^2\right)\right) \approx 2\pi n^2 \frac{\sigma_\Delta^2}{\mu_\Delta^2}. \tag{6}$$

The linearised approximation on the right is valid only for low harmonics and is shown in Figure 4 (black segments). Importantly, this allows for an approximate but very simple estimation of slip, σ_Δ, based on observation of the level of spread in the spectral peaks. This property will be exploited later in the paper.

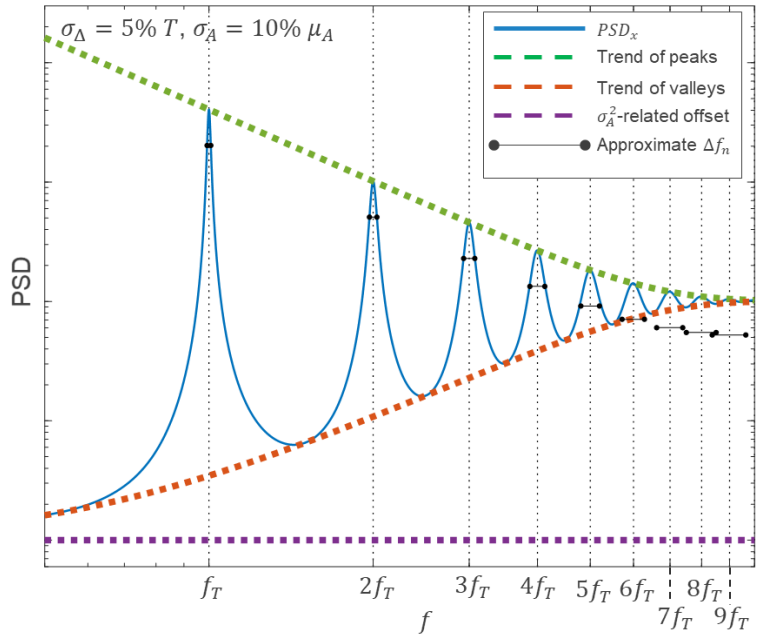

Figure 4: Numerical example of the PSD of the pseudo-cyclostationary model [11]

2.2.4 New mixed model

As with the pseudo-CS model, the mixed model yields a purely random spectrum, with PSD [11]:

$$\mathbb{E}\{PSD_x(f)\} = \frac{|S(f)|^2}{T} \cdot \mu_A^2 \cdot \left\{1 - e^{-\sigma_\tau^2(2\pi f)^2} + \frac{e^{-\sigma_\tau^2(2\pi f)^2}\sinh\left(2\sigma_\Delta^2\pi^2 f^2\right)}{\cosh\left(2\sigma_\Delta^2\pi^2 f^2\right) - \cos(2\pi f/f_T)} + \frac{\sigma_A^2}{\mu_A^2}\right\}. \quad (7)$$

This case has strong similarities with the pseudo-CS model, as shown in the PSDs illustrated in Figure 5, the main difference being the presence of σ_τ (jitter) gives a faster convergence of the amplitude of peaks and valleys with respect to the pseudo-CS case. Note that the same half-power bandwidth approximation used in the pseudo-CS case holds for the estimation of σ_Δ, over which σ_τ has little effect.

The following sections will explain how this bearing model was applied to vibration signals from degradation tests on a laboratory bearing test rig.

3 Methodology

3.1 Experimental set up

Bearing degradation tests were run on a SpectraQuest bearing test rig at UNSW Sydney. The rig is shown in Figure 6, along with a test bearing (6205 grease-lubricated deep-groove ball bearing) at the start of one of the tests. Full details of the experiments can be found in [12, 13]. In this paper, two records will be analysed, Tests 1 and 2. In both cases, the bearings started with a small dimple of 1 mm diameter and 0.1 mm depth on the outer race (right-hand side of Figure 6), and the fault was allowed to propagate to a size of 6-7 mm over the remainder of the tests. Test 1 was run with a horizontal radial load of 10.5 kN applied to the bearing, while in Test 2 the load was 7 kN, representing about 75% and 50% of the rated dynamic load, respectively. Both tests were run at a shaft speed of 30 Hz, but the speed was occasionally reduced to 6 Hz to take vibration measurements, which was done initially every 50,000 cycles and then every 20,000 cycles once the spall had commenced growing. Each vibration measurement was sampled at 51.2 kHz for a duration of 12 s. Test 1 was run for 350,000 cycles, Test 2 for 2 million, and the spall size was measured periodically throughout the test by stopping the rig and disassembling the bearing, before reassembling/reinstalling them

and continuing with the test. A once-per-rev tacho signal was acquired synchronously, allowing for order tracking of the nominally constant speed signals.

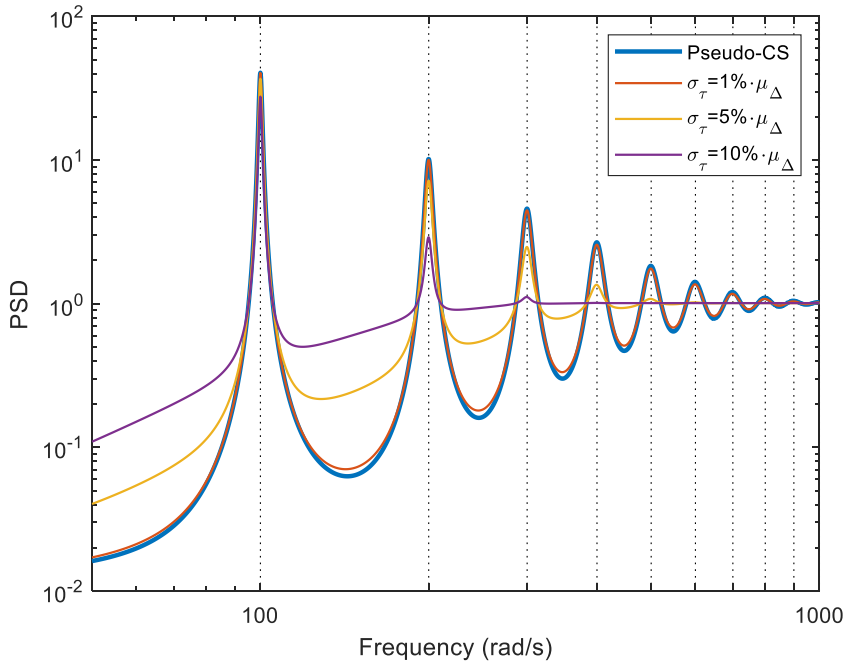

Figure 5: Numerical example of the PSD of the pseudo-CS and mixed models [11]

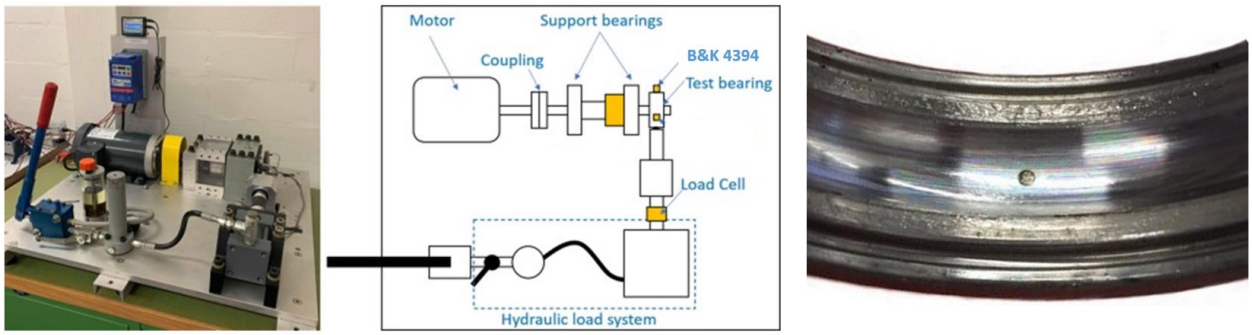

Figure 6: UNSW bearing test-rig and test-bearing (adapted from [13, 14])

3.2 Signal processing

Before fitting the mixed model of Sections 2.1.4 and 2.2.4 to the signals, the latter were first order tracked to account for any small incidental speed fluctuations. The rig tends to produce relatively clear bearing signals with no strong masking agents, and so no further processing was found to be necessary. After order tracking, envelope analysis was conducted to obtain a finer estimate of the actual fault frequency to assist with the fitting.

3.3 Fitting of model parameters

As explained in [11], it is possible to fit the mixed model parameters using maximum likelihood estimation based on the timing of individual pulses identified in the time (or angle) record. However, in this case, while the signals were relatively clean, the pulses were not sufficiently clear and repeatable to allow for a reliable

fitting in the time domain. Accordingly, harmonics of the fault frequency in the order spectrum were investigated for fitting. Such a fitting is based on the property, cf. Section 2.2.3 and Figure 4, that the expanding width of smeared fault 'harmonics' in the spectrum is directly related to σ_Δ, the level of pseudo-CS in the signal. This meant that only the pseudo-CS-related parameters (μ_Δ and σ_Δ) could be investigated, since the CS model parameters (μ_τ and σ_τ) are very difficult to fit in the spectrum. This still provides fertile ground for investigation, however, as it is to be expected that μ_Δ and σ_Δ should both vary with bearing condition, as for example the spall size and surface roughness change, altering frictional forces on the rolling elements. In addition, a strong relationship between the PCS parameters and load was found in [11], and comparison here between the results of Tests 1 and 2 (75% and 50% rated load, respectively) may provide further confirmation of that phenomenon.

The order spectrum of the measured signals was found to be rich in fault frequency harmonics, and after some initial trial and error the 8th harmonic was chosen for fitting in all cases. Generally, a higher harmonic is to be preferred, so long as it protrudes sufficiently from background noise, as it gives a greater number of samples to fit due to the increased spread of harmonics under pseudo-cyclostationarity. Here, the fitting was performed over the order range of $\pm 1\%$ of the component in question, using a mean-squared-error optimisation problem solved using fminsearch in MATLAB. The fitted parameters were the mean fault period μ_Δ (giving a refined estimate of the true fault frequency compared with the initial one from envelope analysis) and PCS level σ_Δ.

An underlying assumption in this analysis is that while the bearings were degrading throughout the tests, the bearing condition (e.g., spall size) remained unchanged in each of the individual records.

4 Results

The results of the $\hat{\mu}_\Delta$ and $\hat{\sigma}_\Delta$ fitting for the records from Test 2 (50% rated load) are shown in Figure 7. The estimated mean fault period, $\hat{\mu}_\Delta$, is shown on the left, with $\hat{\sigma}_\Delta$ plotted on the right. The plot on the left includes two sets of estimates for $\hat{\mu}_\Delta$ – one from the envelope spectrum (SES), the other from the MSE parameter fitting. Both plots also include the measured spall size taken on several occasions throughout the test. Note that there is some quantisation error from the SES-estimated $\hat{\mu}_\Delta$ values; this is because the estimates were simply 'nearest-sample-based' and did not involve any fitting.

While some discontinuities in the $\hat{\mu}_\Delta$ trend can be seen, due to changes from (dis)assembly of the bearing and test rig, there is a clear overall trend in this parameter that matches the evolution in spall size, in particular the sharp jump towards the end of the test, when the level of slip reached almost 1% ($\hat{\mu}_\Delta \approx 1.008$ normalised) and the spall size 6.3 mm.

Overall, it was found that the level of pseudo-cyclostationarity in the signals was very small, and this, combined with the relatively short (12 s) records made obtaining a good fit for $\hat{\sigma}_\Delta$ difficult. This is reflected by the lack of any apparent trend (with spall size or at the inspection points where the rig was disassembled) throughout most of the right-hand plot, which likely just represents random fitting noise. However, at the end of the test, a sudden jump in $\hat{\sigma}_\Delta$ values can be seen, coinciding with the rapid increase in spall size that occurred in that period. Further work will be required to confirm whether this tentative observation does indeed reflect a genuine physical relationship.

Figure 8 shows the fitting results from Test 1 (75% rated load), presented identically to those of Figure 7. Here, more so than in Test 2, sharp discontinuities in $\hat{\mu}_\Delta$ can be seen, illustrating that disassembly and reassembly can give a clearly detectable change in the slip characteristics of the bearing. Note that for each inspection the cages of the bearings were completely separated and the rolling elements removed and then randomly reinstalled, so it is to be expected that this should change the kinematic properties of the bearing. Other than these jumps at the inspection points, it is difficult to discern any clear trend in $\hat{\mu}_\Delta$ throughout the test. Similarly, the plot of $\hat{\sigma}_\Delta$ shows no discernible trend at all.

A comparison of the Test 1 and 2 results offers further evidence (in addition to that presented in [11]) that load is an important factor in the pseudo-CS properties generated by faulty bearings, with more lightly loaded bearings producing more slip and stronger PCS content. For context, note that the radial load applied

to the bearings in this study (50 and 75%) is much greater than in most practical applications, and so the effect is likely to have been understated here. Axial load, not included here, is also likely to be an important 'PCS-enhancing' factor in many applications because it changes the effective rolling diameter of each ball with its position.

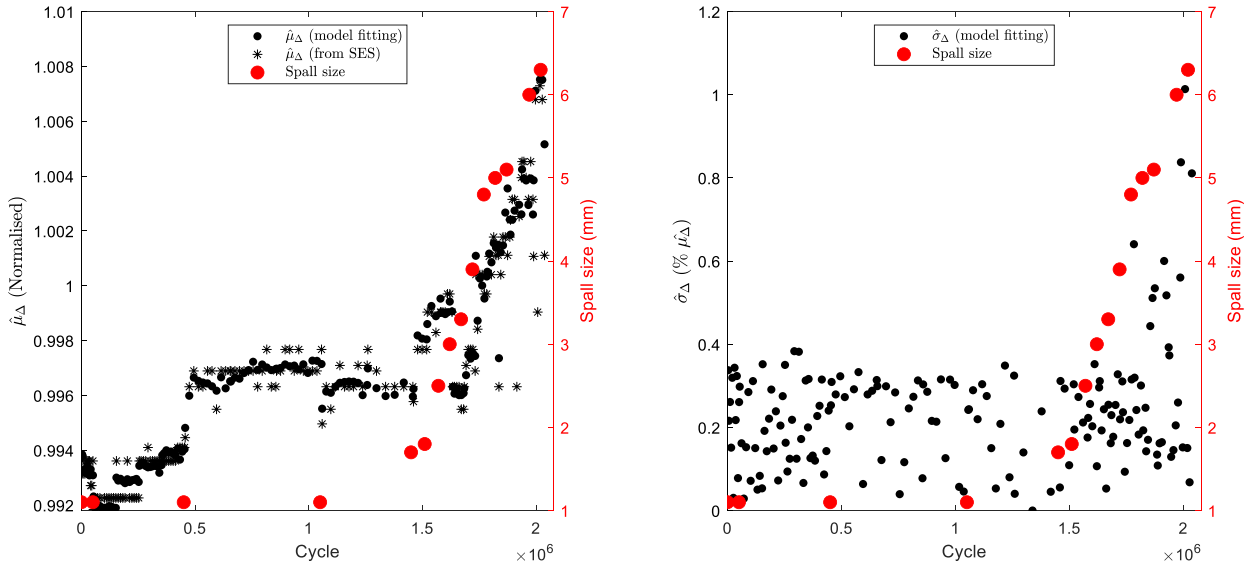

Figure 7: Evolution of estimated pseudo-CS model parameters $\hat{\mu}_\Delta$ and $\hat{\sigma}_\Delta$ throughout Test 2

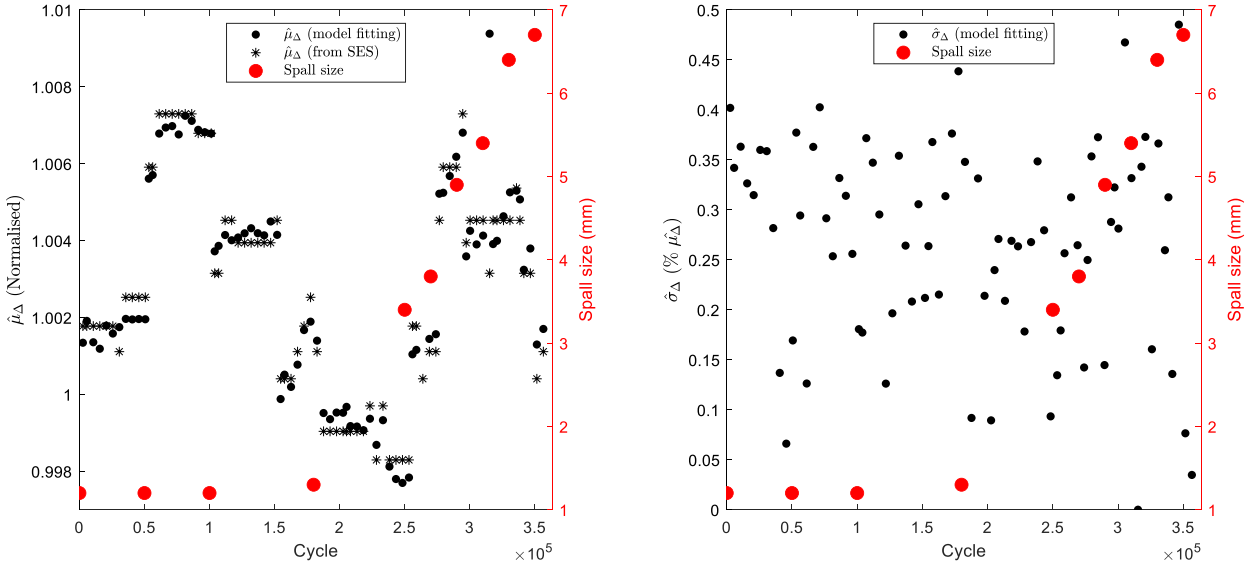

Figure 8: Evolution of estimated pseudo-CS model parameters $\hat{\mu}_\Delta$ and $\hat{\sigma}_\Delta$ throughout Test 1

5 Conclusions and future work

This study took a new look at bearing signal models and explained several key points of existing cyclostationary (CS) and pseudo-cyclostationary (PCS) models, both developed about 20 years ago. A recently proposed mixed CS/PCS signal model was then presented and the fitting of this model's parameters was demonstrated using laboratory data from two degradation tests on a bearing test rig. Specifically, the fitted parameters were the mean fault period, μ_Δ, indicating the level of slip, and σ_Δ, indicating the level of pseudo-cyclostationarity.

The following conclusions can be drawn:

1. The level of pseudo-CS was found to be very small in these tests, and consequently it was difficult to obtain reliable results for the fitting of σ_Δ.
2. The fitting of μ_Δ, on the other hand, was straightforward and yielded meaningful results.
3. In Test 2, where the bearing was run at 50% of its rated load, a strong correlation was found between the mean fault period (μ_Δ), or slip level, and the size of the spall on the bearing outer race.
4. In Test 1, where the bearing was run at 75% of its rated load, this correlation between μ_Δ and spall size was not evident; instead, discontinuities in μ_Δ were found, matching the inspection times when the bearing was removed from the rig and disassembled.
5. It appears that μ_Δ has strong potential as a trending parameter indicative of bearing condition, but the preliminary results here suggest that very heavy radial loads may mask its capabilities.
6. Although σ_Δ, the pseudo-CS level, was difficult to fit in this case, a very tentative finding is that there may be a positive relationship between σ_Δ and spall size. This was only (marginally) apparent for the lower load test, however (Test 2, 50%) and requires further testing and confirmation.

Among the possibilities for future work, the following are worth noting:

1. The cyclostationary model parameters representing ‘jitter’ (from clearance of the rolling elements in the cage) were not investigated in this study. An improved estimation method for these parameters would facilitate further developments and a better understanding of the relationship between cage clearance and bearing condition.
2. Future experimental work will include testing with axial loads, with lower radial loads, and taking longer record lengths to assist with better fitting of the model parameters.

Acknowledgements

This research was partially supported by the Australian Government through the Australian Research Council's Linkage Project LP180101161. The authors would like to thank Hengcheng Zhang for providing the experimental data analysed in the paper.

References

[1] P. D. McFadden, and J. D. Smith, "Model for the Vibration Produced by a Single Point Defect in a Rolling Element Bearing," *Journal of Sound and Vibration*, vol. 96, no. 1, pp. 69-82, 1984.

[2] A. C. McCormick, and A. K. Nandi, "Cyclostationarity in rotating machine vibrations," *Mechanical Systems and Signal Processing*, vol. 12, no. 2, pp. 225-242, 1998, doi: 10.1006/mssp.1997.0148.

[3] C. Capdessus, M. Sidahmed, and J. L. Lacoume, "CYCLOSTATIONARY PROCESSES: APPLICATION IN GEAR FAULTS EARLY DIAGNOSIS," *Mechanical Systems and Signal Processing*, vol. 14, no. 3, pp. 371-385, 2000, doi: http://dx.doi.org/10.1006/mssp.1999.1260.

[4] R. B. Randall, J. Antoni, and S. Chobsaard, "The Relationship Between Spectral Correlation and Envelope Analysis in the Diagnostics of Bearing Faults and Other Cyclostationary Machine Signals," *Mechanical Systems and Signal Processing*, vol. 15, no. 5, pp. 945-962, 2001, doi: 10.1006/mssp.2001.1415.

[5] P. Borghesani, P. Pennacchi, and S. Chatterton, "The relationship between kurtosis- and envelope-based indexes for the diagnostic of rolling element bearings," *Mechanical Systems and Signal Processing*, vol. 43, no. 1–2, pp. 25-43, 2/3/ 2014, doi: http://dx.doi.org/10.1016/j.ymssp.2013.10.007.

[6] A. Mauricio et al., "Bearing diagnostics under strong electromagnetic interference based on Integrated Spectral Coherence," *Mechanical Systems and Signal Processing*, vol. 140, p. 106673, 2020/06/01/ 2020, doi: https://doi.org/10.1016/j.ymssp.2020.106673.

[7] W. A. Smith, R. B. Randall, X. de Chasteigner du Mée and Z. Peng, "Use of Cyclostationary Properties to Diagnose Planet Bearing Faults in Variable Speed Conditions," presented at *the Tenth DST Group International Conference on Health and Usage Monitoring Systems (HUMS)*, Melbourne, Australia, 26-28 February, 2017.

[8] W. A. Smith, P. Borghesani, Q. Ni, K. Wang, and Z. Peng, "Optimal demodulation-band selection for envelope-based diagnostics: A comparative study of traditional and novel tools," *Mechanical Systems and Signal Processing*, vol. 134, pp. 106303, 2019/12/01/ 2019, doi: https://doi.org/10.1016/j.ymssp.2019.106303.

[9] J. Antoni and R. B. Randall, "Differential Diagnosis of Gear and Bearing Faults," *Journal of Vibration and Acoustics*, vol. 124, no. 2, pp. 165-171, 2002. [Online]. Available: http://dx.doi.org/10.1115/1.1456906.

[10] J. Antoni and R. B. Randall, "A Stochastic Model for Simulation and Diagnostics of Rolling Element Bearings With Localized Faults," *Journal of Vibration and Acoustics*, vol. 125, no. 3, pp. 282-289, 2003. [Online]. Available: http://dx.doi.org/10.1115/1.1569940.

[11] P. Borghesani, W. A. Smith, R. B. Randall, J. Antoni, M. El Badaoui, and Z. Peng, "Bearing signal models and their effect on bearing diagnostics," *Mechanical Systems and Signal Processing*, vol. 174, pp. 109077, 2022/07/15/ 2022, doi: https://doi.org/10.1016/j.ymssp.2022.109077.

[12] P. Borghesani, S. Zhuang, H. Zhang, and Z. Peng. *Bearing run-to-failure datasets of UNSW*. doi: 10.17632/h4df4mgrfb.3.

[13] H. Zhang, P. Borghesani, R. B. Randall, and Z. Peng, "A benchmark of measurement approaches to track the natural evolution of spall severity in rolling element bearings," *Mechanical Systems and Signal Processing*, vol. 166, pp. 108466, 2022/03/01 2022, doi: https://doi.org/10.1016/j.ymssp.2021.108466.

[14] H. Zhang, P. Borghesani, W. A. Smith, R. B. Randall, M. R. Shahriar, and Z. Peng, "Tracking the natural evolution of bearing spall size using cyclic natural frequency perturbations in vibration signals," *Mechanical Systems and Signal Processing*, vol. 151, pp. 107376, 2021.